Science World Journal Vol 14 (No 1) 2019
www.scienceworldjournal.org
ISSN 1597-6343
Published by Faculty of Science, Kaduna State University

Full Length Research Article

STRUCTURAL AND DIELECTRIC PROPERTIES OF $Ba(Ti_{0.96}Sn_{0.01}Zr_{0.03})O_3$ PEROVSKITE NANOPARTICLES FABRICATED BY MECHANOCHEMICAL SYNTHESIS ROUTE

[1]Muazu A.*, [2]Suleiman A.B., [3]Ahmadu U., [4]Auwalu I.A., [2]Zangina T., [1]Nura A.

[1]Department of Physics, Federal College of Education (T), Bichi, Kano State, Nigeria.

[2]Department of Physics, Federal University Dutse, Dutse, Jigawa State, Nigeria.

[3]Department of Physics, Federal University of Technology, PM.B. 65, Minna, Nigeria.

[4]Department of Physics, Kano University of Science and Technology, Wudil, Kano State, Nigeria.

*Corresponding Author's Email: hasumm@yahoo.com

ABSTRACT
Lead free Nanocrystalline $BaTiO_3$ doped with Sn and Zr is prepared by a combination of solid-state reaction and high energy ball milling (HBM) technique in a temperature range 30–150 °C, over a frequency range 40 Hz – 1 MHz. A single-phase nanocrystalline sample with ABO_3 type of perovskite structure with cubic symmetry was confirms by XRD diffraction. The crystallite and grain size determined from Scherrer equation and intercept method are 38.2 nm and 46.13 nm respectively. FE-SEM images show samples are dense and have different microstructures with certain amount of porosity. A grain size of 46.13 nm is obtained by using linear intercept method. Room temperature (RT) variation of $\varepsilon'$and tan δ as a function of frequency of the modified BT system has also been studied. Variation of dielectric properties with frequency shows the usual behaviour of dielectric materials i.e decrease of the value of ε' with the increase of frequency. A dielectric anomalies is observed corresponding to phase transitions viz tetragonal to cubic (T_{T-C}) at 70°C. These effect can guide to design the nanostructure for various practical applications of MLCC.

Keywords: Dielectric properties, perovskite, nanoparticles, mechanochemical synthesis.

INTRODUCTION

The demand for the sustainable development of the world and of the environmental and safety concerns has induced a new surge in developing lead-free BT ceramics because it is non-toxic, and environmentally friendly. Barium titanate ($BaTiO_3$) is one of the most extensively studied perovskite (ABO_3) ferroelectric oxides, whose high dielectric constant, low dielectric loss and ferroelectric and piezioelectric properties (Sharma et al., 2015) are largely employed in a variety of electronic devices such as Multilayered Ceramic Capacitors (MLCCs) (Guillon et al., 2012), memory devices (Hoffman et al., 2011), PTC thermistors (Rafiq et al., 2017), and a variety of electro-optic devices (Yang et al., 2012). However, the application in a certain domain of pure $BaTiO_3$ ceramics is limited because of the narrow working temperature-stable range and high dielectric loss (Liu et al., 2016). Substitution of other ions at A, B or in both sites in the $BaTiO_3$ perovskite cells leads to remarkable changes of its functional characteristics. For specific applications such as higher material constants (permittivity, pyro-and piezo-electric constants), better thermal stability in a large temperature range can be induced by isovalent substitution on Ti sites with elements such as: $BaZrxTi1\text{-}xO_3$, (Zhang et al., 2016) Hf, (Fu et al., 2013) Ce, (Padalia et al., 2013) or $BaTi1\text{-}xSnxO_3$ (Ren et al., 2017).

Moreover, technological advances demand miniaturized electronic portable devices with various functions. This leads to high interest from electronic industry in the development of new miniaturized ferroelectric materials used in a wide range of applications of electronic devices such as thinner Multilayer Ceramic Capacitors (MLCC), piezoelectric sensors and actuators. The electrical and piezoelectric properties are reported to be greatly enhanced for BT ceramics which are synthesized from nanopowders (Chandramani et al., 2011; Horchidan et al., 2014). In order to obtain BT powders with a nanometre size, there are varieties of routes for the synthesis of nanoceramic powders such as chemical coprecipitation (Potdar et al., 1999), sol–gel technique (Chen et al., 2011), and hydro thermal synthesis (Xu et al., 2002). However, the high-energy ball milling technique is still considered as a simple and cost effective method for large scale production of nanoceramic powders (Kong et al., 2008; Gusev & Kurlov, 2008). Further, mechanical treatment of ceramic powders can reduce particle size and enable obtainment of nano-structured powders, which are of the main interest in current trend of miniaturization and integration of electronic components (Giri, 1997).

There are several reports (Tan, et al., 2013; Singh & Jiten, 2013) on the influence of solid state or HBM synthesis techniques on the structure, and dielectric properties of Sn or Zr doped $BaTiO_3$ ceramics. To our knowledge, there are not reports about the dielectric properties of Sn and Zr co-doped-$BaTiO_3$ processed by HBM synthesis techniques. In this work, we used the HBM synthesis technique in order to prepare nanocrystalline $BaTiO_3$ co-doped with Sn and Zr ($BaTi_{0.96}Sn_{0.01}Zr_{0.03}O_3$) method to obtain dense ceramics. Dielectric and structural properties of

these materials were investigated and, the possible use for MLCC's and practical application is explored.

EXPERIMENTAL

The solid state and mechanochemical route were followed to synthesize nanocrystalline $Ba(Ti_{0.96}Sn_{0.01}Zr_{0.03})O_3$ ceramic. The raw materials (powders) were analytical grade of oxide precursors of AR $BaCO_3$ (99.9 %), TiO_2 (99.9+ %), SnO_2 (99.9 %), and ZrO_2 (99.9 %). The stoichiometric value of the oxides were weighed according to the nominal composition and mixed via ball-mill for 12 h in alcohol. The mixture was first dried in oven and calcined at 1050oC for 4 h in aluminum crucibles. The calcined powders were mechanically activated by high-energy ball mill in isopropyl alcohol as wetting medium using SPEX 8000 Mixer/Mills at room temperature for 7 h. The milling process was stopped for 15 min after every 60 min of milling in order for the system to cool down. The resultant slurry was dried in an oven at 90oC for 24 h. The dried powder was compacted at 49033.25 N/m2 to make pellets of size 10 mm in diameter and 1 mm thickness using polyvinyl alcohol (PVA) as a binder. The pressed pellets in form of disks were sintered at temperatures of 1190oC for 2h.

Characterization

The crystal structure and phase analyses was identified using X-ray diffractometer (XPERT-PRO) with monochromatic Cu Kα radiation at λ = 1.54178 Å at 40 kV/40 mA in the 2θ range from 20◦ to 80◦. The microstructural studies were carried out by using field emission scanning electron microscopy (FESEM, JEOL 7600F, U. S. A), operated at a voltage of 15 kV and images captured at 5 kV with magnification of × 100,000. For electrical measure silver paste was painted on the polished sample as the electrodes and fired at 550oC for 15 min. The frequency (40 Hz − 1MHz) and temperature (30 to 400oC) dependent dielectric analysis was evaluated using Impedance Analyzer (Agilent 4294A, Japan) at an oscillation amplitude of 500 mV connected to a computer.

The lattice constant of all the sample are calculated using the equations.

$$a^2 = \frac{\lambda}{2}\frac{[(h^2+k^2+l^2)]}{sin^2\theta} \quad (1)$$

where λ is the wavelength of X-ray (λ =1·54178 Å), θ is the Bragg angle and hkl are the Miller indices of the corresponding planes.

The crystallite size of the powders (D) calculated from XRD data by the Scherer's formula (Cullity, 1978) from XRD data given as

$$D = \frac{0.98\lambda}{\beta\, cos\theta} \quad (2)$$

where D is the crystalline size, 0.98 is the crystalline shape factor, β is the full width at half maxima (FWHM) at Bragg's angle (2θ), and, λ is the X-ray wavelength of CuKα (λ = 1·54178 Å).

RESULTS AND DISCUSSION

Microstructural and morphological analysis

Figure 1a shows the room temperature XRD pattern of $Ba(Ti_{0.96}Sn_{0.01}Zr_{0.03})O_3$ ceramic. It is seen that the composition is of single phase perovskite structure without any trace of impurity in the background. The non-splitting of (200) and (002) peaks (Buttner & Maslen, 1992) at diffraction angle of 44 to 46.5o clearly show that the crystal structure of Ba (Ti0.96Sn0.01Zr0.03) O3 was assigned to the cubic phase with Pm-3m space group verified from JCPDS database (card no 98-000-2020), as reported by other researchers (Burtr & Jianping, 2001; Lazarevi et al., 2010). The lattice parameters, crystalline size and unit cell volume were estimated and presented in Table 1. From table 1, the obtained lattice parameter were a = b = c = 4.014849 Å confirming the cubic structure. The crystallite size of 38.2 nm for $Ba(Ti_{0.96}Sn_{0.01}Zr_{0.03})O_3$ is similar to the one obtained by (Attara et al., 2017). Figure 1a inset shows the typical FESEM micrographs of $Ba(Ti_{0.96}Sn_{0.01}Zr_{0.03})O_3$ ceramics sintered at 1190oC for 2 hrs. It can be seen that the sintered ceramic sample is dense, the grains are indistinguishable and have varying microstructures with presence of voids. The presence of voids in the FESEM image indicate that the pellet have certain amount of porosity. The grain size and grain boundary are observed very clearly. The average grain size of $Ba(Ti_{0.96}Sn_{0.01}Zr_{0.03})O_3$ ceramics determined by using linear intercept technique (Abrams, 1971) is found to be 46.13 nm.

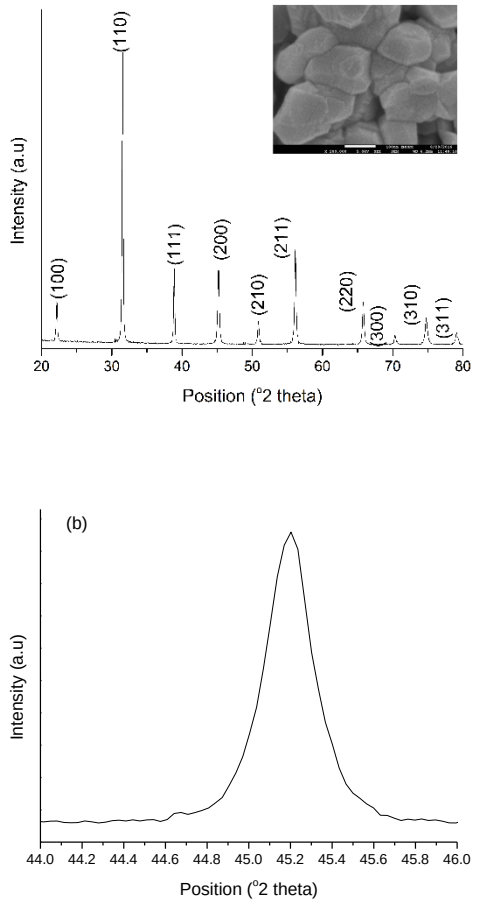

Figure 1: (a) Room temperature XRD Patterns and inset FESEM micrograph at × 200000 magnification (b) Enlarged XRD Patterns from 44 to 46o of nanocrystalline

$Ba(Ti_{0.96}Sn_{0.01}Zr_{0.03})O_3$ ceramics sintered at 1190oC

Table 1: Lattice parameter and crystallite size of $Ba(Ti_{0.96}Sn_{0.01}Zr_{0.03})O_3$ ceramic.

Sample	Ba(Ti0.96Sn0.01Zr0.03)O3
a (Å)	4.014849
b (Å)	4.014849
c (Å)	4.014849
c/a	1.00000
Volume (Å3)	64.40
Crystallite size (nm)	38.2

Frequency and temperature dependence of real dielectric permittivity (ε') and dielectric loss ($\tan\delta$).

Fig. 2a and 2b shows the frequency dependence of real dielectric permittivity (ε') and dielectric loss ($tan\ \delta$) as a function of temperature for Sn and Zr doped BT sintered samples synthesized by Mechanohemical route. The ε' is higher at low frequency and decreases with the increase in frequency. The fall in ε' arises from the fact that polarization does not occur instantaneously with the application of the electric field, which is further due to the inertia of the dipoles and the delay in response towards the impressed alternating electric field leads to dielectric loss and decline in ε' (Tkacz- miech et al., 2003). At low frequencies, all types of polarizations contributes and as the frequency is increased, polarizations with large relaxation times cease to respond and hence the decrease in ε' (Chopra et al., 2004). At lower frequencies ε' is maximum because the contributions from the space charge polarization is large (Singh et al., 2002). The space charge polarization arises by the accumulation of charges mainly due to vacancies of oxygen at the grain boundaries and at the electrode interface (Griffiths, 1998). At higher frequencies, contributions from the polarizations having high relaxation time ceases resulting in the decrease in ε' (Kittel, 1995). The same type of frequency-dependent dielectric behaviour is found in all other ferroelectric ceramic systems (Jaffe et al., 1972; Lines & Glass, 1979).

Figure 2b plots the frequency dependence of dielectric loss ($tan\ \delta$) of the $Ba(Ti_{0.96}Sn_{0.01}Zr_{0.03})O_3$ ceramic at various temperatures. The dielectric loss decreases with increasing frequency and the decrease is more pronounces at higher temperatures but show a broad step and a broad maximum in the frequency range 103 < f < 105 Hz, respectively. A peak in the dielectric loss occurs when $\omega\tau = 1$, that is when the relaxation frequency matches the applied frequency and are seen to shift towards higher frequency with increase in temperature (Mansour & Elkestawy, 2011). The loss peaks and their shift with temperature suggest a thermally activated dielectric relaxation process (Mohan et al., 2010). Dielectric loss (tan δ) is owed to the relaxation of space charge polarization. A direct elucidation is that the peak height of tan δ is decided by the relaxation strength. The minimum loss is obtained at 130oC is 0.019.

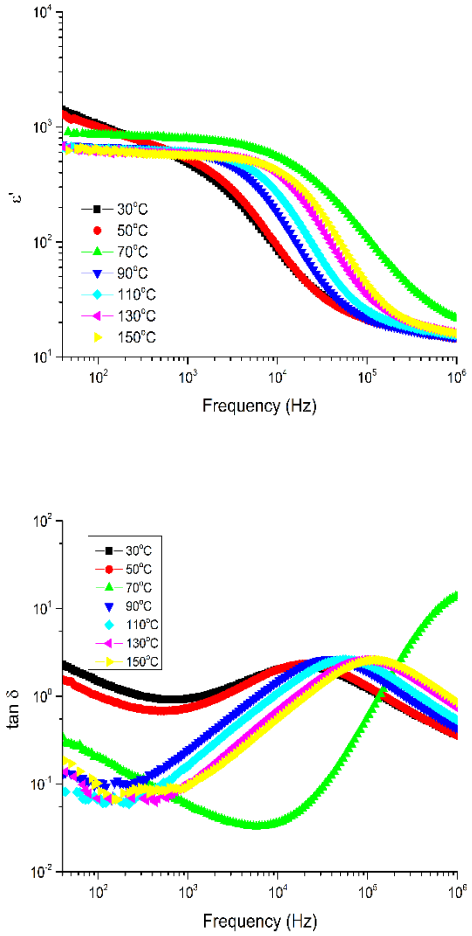

Figure 2: Variation of (a) real dielectric permittivity (ε'), and (b) imaginary dielectric permittivity (ε'') at various temperatures of $Ba(Ti_{0.96}Sn_{0.01}Zr_{0.03})O_3$ ceramic.

Figure 3 shows the variation of real dielectric permittivity (ε') and loss tangent ($tan\ \delta$) as a function of temperature (30 to 150oC) of $Ba(Ti_{0.96}Sn_{0.01}Zr_{0.03})O_3$ ceramic sintered at 1190°C, measured at 40Hz, 100Hz, 1 kHz, 10 kHz, 100 kHz, and 1 M Hz. The dielectric constant decreases with an increase in frequency. It is seen that the $Ba(Ti_{0.96}Sn_{0.01}Zr_{0.03})O_3$ undergoes a sharp ferroelectric to paraelectric (tetragonal to cubic) transition at 70°C, the ferroelectric-ferroelectric transition (orthorhombic to tetragonal) may have transition below the room temperature. At frequency of 40Hz, 100Hz, ε' decreases with decrease of frequency and temperature and on further increase of the temperature ε' decreased and becomes frequency independent. At higher frequency of 1 kHz, 10 kHz, 100 kHz, and 1 MHz the values of ε' increases with the increase in temperature and transition temperature (Tc) was found to be around 70oC. The value of Tc is nearly the same for the system synthesized by solid state reaction route. It is clear that the T_c (70°C) has shifted to a lower temperature. A similar trend was obtained by others workers (T_c, 95oC) (Long et al., 2017). Curie

temperature is that at which ferroelectric materials are changed from ferroelectric to non-ferroelectric. Generally, for bulk $BaTiO_3$ material, it is 120–130°C. The lowering of T_c may be attributed to various factors such as the electrostrictive strain (Rossetti et al., 1991), two-dimensional compressive stress (Hayshi, 1973) in the direction of ferroelectric, photomechanical effect (Lemieux, 2005), mechanical compression along c-axis and tension along a-axis (Kuwabara et al., 1997). Also, Uchino (2000), suggested that with decreasing grain size, T_c was shifted downward through room temperature, eventually tending toward 0 K at some critical particle size. The observed trend of T_c may be due to a combination of various factors mentioned above. In addition, the maximum in the dielectric loss ((Fig. 4(e)) coincides with the maximum in the ε', indicating that the $Ba(Ti_{0.96}Sn_{0.01}Zr_{0.03})O_3$ sample undergoes a structural phase transition which corresponds to the cubic-tetragonal phase. It can be seen that $Ba(Ti_{0.96}Sn_{0.01}Zr_{0.03})O_3$ exhibits T_c of 70oC. Hence, good material for MLCC and practical applications.

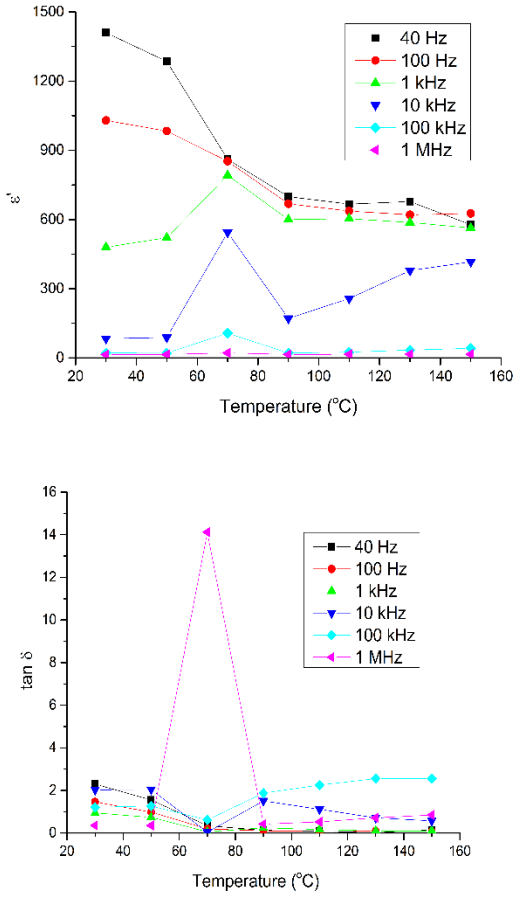

Figure 3: Temperature dependence of (a) real permittivity (ε') and (b) loss tangent ($tan\ \delta$) at different frequency of $Ba(Ti_{0.96}Sn_{0.01}Zr_{0.03})O_3$ ceramic.

CONCLUSION

Nanocrystalline $Ba(Ti_{0.96}Sn_{0.01}Zr_{0.03})O_3$ ceramic powders were successfully obtained from mixed oxide method by two different synthesis techniques such as solid state and HBM. XRD studies revealed cubic structure without showing any secondary phase. FE-SEM images show sample is dense and have different microstructures with certain amount of porosity. The frequency dependent dielectric study reveals a normal ferroelectric behavior in the material. It is found that HBM and Tin/Zirconium concentration has significant influence on structural and dielectric properties of $Ba(Ti_{0.96}Sn_{0.01}Zr_{0.03})O_3$. The temperature dependent dielectric study shows T_c value of 70oc. This work provide valuable information for $Ba(Ti_{0.96}Sn_{0.01}Zr_{0.03})O_3$ ceramic and fabrication of MLCCs and practical application.

REFERENCES

Abrams, H. (1971). Grain size measurement by the intercept method. *Metallography*, 4(1): 59-78. https://doi.org/10.1016/0026-0800(71)90005-X.

Attara, A.S., Sichanib, E.S., Sharafi, S. (2017). Structural and dielectric properties of Bi-doped barium strontium titanate nanopowders synthesized by sol–gel method. *Journal of material research and technology*, 6(2):108–115.

Burtr, L. and Jianping, Z. (2001). Preparation, structure evolution and dielectric properties of $BaTiO_3$ thin films and powders by an aqueous sol–gel process. *Thin Solid Films*, 388:107-133.

Buttner, R. H. and Maslen, E. N. (1992). Structural parameters and electron difference density in $BaTiO_3$. *ActaCrystallographica, Section B*, 48:764 – 769.

Chandramani, S. K., Natha, A.K., Laishramb, R., Thakurb, O.P. (2011). Structural, electrical and piezoelectric properties of nanocrystalline tin-substituted barium titanate ceramics. *Journal of Alloys and Compound*. 509, 2597.

Chen, X.Y., CAI, W., Fu, C.L., Chen, H.Q., Zhang, Q. (2011). Synthesis and morphology of Ba(Zr0.20Ti0.80)O3 powders obtained by sol–gel method, *Journal of Sol–Gel Science and Technology*, 57, 149–156.

Chopra, S., Sharma, S., Goel, T.C., Mendiratta, R.G. (2004). Effect of Annealing temperature on the Microstructure of chemically deposited Ca modified Lead Titanate Effect thin films. *Applied Surface Science*. pp. 230-207.

Cullity, B.D. (1978). Elements of X-Ray Diffraction, Addison Wesley, Boston, Mass, USA, 2nd edition.

Fu, C., Chen, Q., Cai, W., Chen, G., Deng, X. (2013). Effect of Zr doping on the microstructure and electric properties of Ba Hf Ti O ceramics. *Journal of Material science: Material electronics*, Vol: 24:1303–1307 DOI10.1007/s10854-012-0924-1.

Giri, A. K., (1997). Nanocrystalline materials prepared through crystallization due to instability in amorphous materials after grinding. *Advanced Materials*, 9:163–166.

Griffiths, D.J. (1998). Introduction to Electrodynamics, 3rd edition, Prentice Hall (1998).

Guillon, O., Chang, J., Schaab, S., Kang, S.J.L. (2012) *Journal of the American Ceramic Society*, 95, 2277.

Gusev, A.I., and Kurlov, A.S. (2008). *Nanotechnology,* 19, 265302-1~8.

Hayshi, M. (1973). Shift of Curie temperature of Barium Titanate Due to Two-Dimensional Pressure. *Journal of the Physical Society of Japan*.34(6) 1561-1562.

Hoffman, J., Hong, X., Ahn, C.H. (2011). *Nanotechnology* 22,254014.

Horchidan, N., Ianculescu, A.C., Vasilescu, C.A., Deluca, M., Musteata, V., Ursic, H., Frunza, R., Malic, B., Mitoseriu, L. (2014). Multiscale study of ferroelectric–relaxor crossover in BaSnxTi1−xO3 ceramics. *Journal of the European Ceramic Society* 34, 3661–3674.

Jaffe, B., Cook, W., and Jaffe, H. (1972). *Piezoelectric ceramics,* Academic Press, New York: pp. 53-91.

Kittel, C. (1995). *Introduction to Solid-state Physics*. Wiley, New York.

Kong, L.B., Zhang, T.S., Ma, J., and Boey, F. (2008). Progress in synthesis of ferroelectric ceramic materials via high energy mechanochemical technique, *Progress in Material Science*, 53 (2): 207–322.

Kuwabara, M., Matsuda, H., Kurata, N., Matsuyama, E. (1997). Shift of the Curie point of Barium Titanate Ceramics with Sintering Temperature. *Journal of American Ceramics Society*. 80(10), 2590–96. https://doi.org/10.1111/j.1151-2916.1997.tb03161.x.

Lazarevi, Z. Z., Vijatovi, M. Z., MitroviDohcevi, R., Rom, N. Z., Rom, M. J., Paunovi, N., and Stojanovi, B.D. (2010). The characterization of the barium titanate ceramic powders prepared by the Pechini type reaction route and mechanically assisted synthesis. *Journal of the European Ceramic Society,* 30:623–628.

Lemieux, R.P. (2005). Photoswitching of ferroelectric liquid crystals using photochromic dopants. *SoftMatter1*, 348-354.

Lines, M. E., and Glass, A. M. (1979). Principles and Applications of Ferroelectrics and Related Materials, Oxford, Clarendon.

Liu, S.H., Xue, S.X., Xiu, S.M., Shen, B., Zhai, J.W. (2016). Scientific Reports. 6, 26198.

Long, P., Liu, X., Long, X., Yi, Z. (2017). Dielectric relaxation, impedance spectra, piezoelectric properties of (Ba, Ca)(Ti, Sn)O_3 ceramics and their multilayer piezoelectric actuators. *Journal of Alloys and Compounds,* doi: 10.1016/j.jallcom.2017.02.237.

Mansour, S.F., Elkestawy, M.A. (2011). A comparative study of electric properties of nano-structured and bulk Mn–Mg spinel ferrite. *Ceramic International.* 37(4): 1175-1180.

Mohan, V.M., Qiu, W., Shen, J., and Chen, W. (2010). Electrical properties of poly(vinyl alcohol) (PVA) based on LiFePO4 complex polymer electrolyte films, *Journal of Polymer Research* 17(1),143.

Padalia, D., Bisht, G., Johri, U.C., and Asokan, K. (2013). Fabrication and characterization of cerium doped barium titanate/PMMA nanocomposites. *Solid-state Sciences*, 19:122-129.

Potdar, H.S., Deshpande, S.B., and Date, S.K., (1999). Chemical coprecipitation of mixed (Ba+ Ti) oxalates precursor leading to BaTiO3 powders. *Materials chemistry and physics*, 58(2): 121-127.

Rafiq, M.A., Khan, M.T., Muhammad, Q.R., Waqar, M., Ahmed, F. (2017). Impedance analysis and conduction mechanism of Ba doped $Mn_{1.75}Ni_{0.7}Co_{0.52}xCu_{0.05}O_4$ NTC thermistors. *Applied Physica A*,123:589.DOI10.1007/s00339-017-1192-y.

Ren, P., Liu, Z., Wang, Q., Peng, B., Ke, S., Fan, H., and Zhao, G. (2017). Large nonlinear dielectric behavior in BaTi1−xSnxO3. *Scientific Reports,* 7, DOI: 10.1038/s41598-017-07192-x.

Rossetti, G.A., Eric, C, L., Kushida, K. (1991). Stress induced shift of the Curie point in epitaxial $PbTiO_3$ thin films *Applied Physics Letters*.59 (20) 2524.

Sharma, S., Shamim, K., Ranjan, A., Rai, R., Kumari, P., and Sinha, S. (2015), Impedance and modulus spectroscopy characterization of lead free barium titanate ferro-electric ceramics, *Ceramics International*, 41: 7713-7722 http://dx.doi.org/10.1016/j.ceramint.2015.02.102.

Singh, A.K., Goel, T.C., Mendiratta, R.G., Thakur, O. P., Prakash, C. (2002). Dielectric properties of Mn-substituted Ni–Zn ferrites. *Journal of Applied Physics,* 91, 6626-6630.

Singh, K.C., and Jiten, C. (2013). Size effect on piezoelectric properties of Barium stannate titanate ceramic prepared from nanoparticles. *Journal of Material science: Material electronics*, 24:4247-4252.

Tan, Y.Q., Zhang, J.L., and Wang, C. L. (2013). High piezoelectric properties and good temperature stabilities of CuO-modified $Ba(Ti_{0.96}Sn_xZr_{0.04-x})O_3$ ceramics, *Journal of Advanced Dielectrics,* 3(2):1350014.

Tkacz- miech, K., Kole, A., Ptak, W. S. (2003). *Solid State Communications*, 127 -557.

Uchino, K. (2000). *Ferroelectric Devices*, Marcel Dekker, New York.

Xu, H., Gao, L. Goo, J. (2002). Hydrothermal synthesis of tetragonal barium titanate from barium chloride and titanium tetrachloride under moderate conditions. *Journal of the American Ceramic Society*, 85,727–729.

Yang, X., Su, X., Shen, M., Zheng, F., Xin, Y., Zhang, L., Hua, M., Chen, Y., Harris, V.G. (2012). *Advance Material*. 24, 1202.

Zhang, Y., Li, Y., Zhu, H., Fu, Z., Zhang, Q. (2016). Sintering temperature dependence of dielectric properties and energy-storage properties in (Ba, Zr)TiO3 ceramics. *Journal of Material science: Material electronics,* DOI10.1007/s10854-016-5552-8.